Thrust chamber modelling for the analysis of liquid rocket engine transients

Marco Leonardi*[1], Francesco Di Matteo†[2], Johan Steelant‡[2], Francesco Nasuti§[1], and Marcello Onofri¶[1]

[1]*University of Rome "La Sapienza", Dip. Ingegneria Meccanica e Aerospaziale, Rome, Italy*
[2]*ESA-ESTEC, Aerothermodynamic & Propulsion Analysis Section, Noordwijk, The Netherlands*

Abstract

Modelling the typical transient phases of a Liquid Rocket Engine (LRE) requires a suited level of detail, in order to reproduce all the characteristic phenomena inherent to the flow evolution of a combustion chamber. When dealing with the typical unsteady operational conditions of a rocket engine, such as start-up and shut-down phases, a detailed description of the driving physical processes, e.g. wave propagation and combustion, is crucial. From a system point of view the LRE components need to be modelled in an accurate way to correctly simulate the mutual component influence on the overall engine performance. Furthermore, in the quest for a satisfactory level of reliability, one should also aim for simplified sub-models assuring a reasonable computational time which is a desired feature for design iterations. EcosimPro is an objected oriented tool in which, thanks to the propulsion library ESPSS, all the typical components of a liquid rocket engine (tanks, turbo machinery, feeding lines, valves, gas generator/preburner, combustion chamber, etc.) are modelled to study both steady states and transients.

In this paper a quasi one dimensional component to analyse liquid rocket engine combustion chambers in chemical non equilibrium is presented. The numerical approach consists of a finite volume formulation of the unsteady quasi one dimensional Euler equations for multispecies flow coupled with finite-rate chemistry. The inviscid convective fluxes are treated with two schemes, specifically formulated for multispecies flows: the approximate Riemann solver of Roe and the AUSM$^+$-up. Both the schemes are implemented with a spatial accuracy up to the third order by means of the Monotonic Upstream Centered Scheme for Conservation Laws (MUSCL). The mechanism presented consists of six species and eight reactions for the combustion of hydrogen and oxygen. The time integration is left to the DASSL solver embedded in EcosimPro. The DASSL is an implicit solver able to deal with the stiffness introduced by the source terms representing the finite-rate chemistry.

After the description of the numerical model, some validation test cases for the schemes and the finite-rate chemistry mechanism are presented. Finally the component is tested on the Space Shuttle Main Engine (SSME) Main Combustion Chamber (MCC) and the results are compared against those obtained with an already validated software. The tests show that the component is able to reach the expected steady-state solution in terms of both evolution of the thermodynamic properties and mixture composition.

*Ph.D Student, marco.leonardi@uniroma1.it
†Propulsion Engineer, francesco.di.matteo@esa.int
‡PhD, Propulsion and Aerothermodynamic Engineer, johan.steelant@esa.int
§Associate Professor, francesco.nasuti@uniroma1.it
¶Professor, marcello.onofri@uniroma1.it

NOMENCLATURE

$\widehat{\lambda}_i$	i-th average eigenvalue, m/s
$\dot{m}$	mass flow rate, kg/s
γ	third-body efficiency
ν'	stoichiometric coefficient for reactants
ν''	stoichiometric coefficient for products
ω_i	species rate of production, kg/s
ρ	mixture density, kg/m^3
ρ_i	species densities, kg/m^3
$\widehat{\alpha}_i$	i-th average wave strength
$\widehat{\epsilon}_i$	i-th average eigenvector
A	cross section area, m^2
C_i	species concentration, $kmol/m^3$
E	total energy per unit mass, J/kg
E_a	activation energy, cal/mol
H	total enthalpy per unit mass, J/kg
k_b	backward rate constant, m–kg–K
k_f	forward rate constant, m–kg–K
M_w	species molecular weight, g/mol
N_r	number of reactions
N_s	number of species
p	pressure, Pa
q	heat flux, W/m
R	universal ideal gas constant, $J/(kmol \cdot K)$
T	temperature, K
u	velocity, m/s
y_i	species mass fractions

1 Introduction

The analysis of Liquid Rocket Engines (LRE) has been conducted during the years with a wide variety of tools at different levels of detail. From a system point of view, coupling different subsystems of the LRE to analyse their mutual influence is a crucial step for both design and off-design analyses. A large number of components is usually involved in the simulation of a complete propulsion system, hence simplified sub-models are commonly preferred in order to ensure an adequate level of reliability with a reasonable computational time. Ecosimpro [1] is an object oriented simulation tool that allows the user to extend the analysis of LRE to the whole propulsion system, using a number of different components that, once connected to each other, enable both steady and transient analyses. Propulsion systems can be investigated by the European Space Propulsion System Simulation (ESPSS) [2] library, which is embedded in the EcosimPro platform. Among all the components introduced with ESPSS we are here interested in the combustion chamber. The presently available combustion chamber component consists, in turn, of two different sub-components. The first one simulates the combustion chamber up to the throat and is capable to deal with the transient behaviour of the flow thanks to an unsteady formulation of the conservation equations. In this first part of the combustion chamber the flow is considered in chemical equilibrium. Instead, the divergent part is modelled with a component that simulates the steady-state expansion by means of analytic correlations for a flow in either frozen or equilibrium conditions. Though for general transient simulations this level of detail is sufficient [3],[4], it may bring to some inaccuracy when chemical non-equilibrium plays a significant role. In this paper an unsteady component able to describe the evolution of a multi-species flow in chemical non-equilibrium is presented. To retain the underlying lightweight philosophy of EcosimPro a quasi one dimensional formulation has been adopted and two different schemes for the convective fluxes have been implemented: the approximate Riemann solver of Roe [5] and the AUMS+_up [6]. The time integration is left to the embedded DASSL [7], an implicit solver able to handle the stiffness introduced by the combustion terms. In the first part of the paper a review of the implemented models is given, then some validation tests are shown for both the convective and the reactive terms. After this first validation procedure, results obtained for the SSME MCC are compared with those obtained from the Two-Dimensional Kinetic software [8].

2 Physical and Mathematical Model

When dealing with an engineering tool it is necessary to reduce the computational time to allow for fast computations. The present component is hence based on a quasi one dimensional finite volume formulation of the conservation equations for multi-species and inviscid flows. Multi-species flows are usually treated describing the evolution of the single species in terms of either partial densities or species concentrations. In the present work the system of equations consists of N mass balance equations written in terms of partial densities plus a momentum equation and an energy equation (1) (2), where N is the number of species:

$$\frac{\partial \boldsymbol{u}}{\partial t} + \frac{\partial \boldsymbol{f}(\boldsymbol{u})}{\partial x} = \boldsymbol{S}(\boldsymbol{u}) \tag{1}$$

with

$$\boldsymbol{u} = A \begin{pmatrix} \vdots \\ \rho_i \\ \vdots \\ \rho u \\ \rho E \end{pmatrix} \qquad \boldsymbol{f}(\boldsymbol{u}) = A \begin{pmatrix} \vdots \\ \rho_i u \\ \vdots \\ \rho u^2 + p \\ \rho u H \end{pmatrix}$$

$$\boldsymbol{S}(\boldsymbol{u}) = \begin{pmatrix} \vdots \\ \omega_i \\ \vdots \\ p A_x \\ q \end{pmatrix} \tag{2}$$

The inviscid fluxes $\boldsymbol{f}(\boldsymbol{u})$ are treated by means of two different schemes. The first one is the approximate Riemann solver of Roe, specifically formulated for multi-component gas flows [9]. This scheme has been chosen to retain the same approach already followed in the Tube and Pipe components of the FLUID_FLOW_1D library in ESPSS, where the Roe solver is implemented aside of a centered scheme. It is worth pointing out that the present scheme is not a simple extension of the one embedded in ESPSS but a new scheme, specifically dedicated to multi-component gas mixtures.

The Roe's scheme solves exactly an approximate Riemann problem. The approximation is based on the introduction of a constant Jacobian defined as:

$$\boldsymbol{A(u)} = \frac{\partial \boldsymbol{f(u)}}{\partial \boldsymbol{u}} \tag{3}$$

The Jacobian is required to satisfy a set of three properties, but is not needed to calculate the final fluxes. In order to compute the Roe inviscid fluxes only the expressions for the wave strengths, eigenvalues and eigenvectors of the Jacobian are required:

$$\mathbf{f}_{1/2} = \frac{1}{2}(\mathbf{f}_R + \mathbf{f}_L) + \sum_i^m |\widehat{\lambda}_i| \widehat{\alpha}_i \widehat{\epsilon}_i \tag{4}$$

where the subscript $1/2$ indicates the generic interface and the subscripts L and R stand for the left and right state with respect to the interface. The sum operator is performed over the total number of the species m and all the quantities are calculated at the average Roe state as reported in [5]. The average Roe state must be defined for any particular case, e.g. two-phase flow or multi-species flow, making it cumbersome to extend to different flow types. For this reason, and in the

search for a less computationally expensive scheme, also the AUSM$^+$-up scheme [6] has been implemented.

The AUSM$^+$-up is an extension of the original AUSM [10] able to deal with all fluid speeds. The AUSM scheme considers the inviscid fluxes as the sum of a convective term and a pressure term (5).

$$\boldsymbol{f} = \boldsymbol{f}^c + \boldsymbol{P} \tag{5}$$

For the specific multi-species problem these terms are:

$$\boldsymbol{f}^c(\boldsymbol{u}) = \dot{m} \begin{pmatrix} \vdots \\ y_i \\ \vdots \\ u \\ H \end{pmatrix}, \quad \boldsymbol{P} = \begin{pmatrix} \vdots \\ 0 \\ \vdots \\ p \\ 0 \end{pmatrix} \tag{6}$$

Here the convective term $\boldsymbol{f}^c(\boldsymbol{u})$ is written as the product of a common scalar mass flux and the passive scalar quantities indicated in the brackets. The second term $\boldsymbol{P}$ contains only the static pressure. The inviscid fluxes at each interface can then be rewritten as,

$$\boldsymbol{f}^c(\boldsymbol{u}) = \boldsymbol{f}_{1/2} = \dot{m}_{1/2}\vec{\phi}_{L/R} + \boldsymbol{P}_{1/2} \tag{7}$$

where the subscript $1/2$ indicates the generic interface and $\vec{\phi}_{L/R}$ is determined in a simple upwind fashion. An interesting aspect of this formulation is how the common mass flux is treated. Usually it is expressed in terms of a common numerical speed of sound:

$$\dot{m}_{1/2} = u_{1/2}\rho_{1/2} = a_{1/2}M_{1/2}\rho_{1/2} \tag{8}$$

The definition of this scalar quantity is crucial in the formulation of the scheme. Different approaches have been proposed during the years and the one adopted in the present work is inferred from [11]. Once the common mass flux is defined, the numerical flux terms in (2) are derived by a simple upwind selection [6].

For both the implemented schemes a high order reconstruction based on the Monotonic Upstream Centered Scheme for Conservation Laws scheme (MUSCL) has been adopted. In EcosimPro the MUSCL was already implemented for the two phase flow in the FLUID_FLOW library. This formulation is here extended to deal with multi-species flow.

A mixture of prefect gases is considered and the thermodynamic properties of the single species are retrieved from a polynomial reconstruction. The ESPSS library embeds dedicated functions to calculate enthalpy, entropy and heat capacity at constant pressure from the thermodynamic database of [12]. These functions are directly used in the present component. Once the property for the single species is calculated, the mixture enthalpy, entropy and heat capacity at constant pressure are obtained summing each species property multiplied with the respective mass fraction.

2.1 Finite Rate Model

The terms ω_i in the source term vector of equation (2) represent the rate of production of the generic species i. In the present analysis this source terms are modelled in a classical finite-rate approach. In each of the continuity equations the source terms are then defined as:

$$\omega_i = M_w \sum_{j=1}^{N_r} \Gamma(\nu''_{j,r} - \nu'_{j,r}) \times \\ \times (k^r_f \prod_{i=1}^{N_s} [C_{i,r}]^{\nu'_{i,r}} - k^r_b \prod_{i=1}^{N_s} [C_{i,r}]^{\nu''_{i,r}}) \tag{9}$$

Where Γ represents the effect of the third bodies

$$\Gamma = \sum_{i=1}^{N_s} \gamma C_j \tag{10}$$

The forward rate coefficients are expressed in the common Arrhenius form

$$k_f = AT^n exp(-E_a/RT) \tag{11}$$

Once the forward rate constant is known the backward rate constant is computed from the thermodynamic equilibrium. In the present component two different schemes are implemented: a global mechanism for methane/oxygen combustion and a reduced mechanism for hydrogen/oxygen combustion. The latter is the one considered in the present study. The reduced mechanism for hydrogen/oxygen involves six species and consists of eight different reactions with third body effects. The proposed scheme is inferred from the Two Dimensional Kinetics (TDK) solver [8], that will be used in the validation section to compare the results obtained with EcosimPro. The reactions reported in Table 1 are taken from [13] making exception for the dissociation of hydroxide and molecular oxygen, taken respectively from [14] and [15].

	A	E_a	n
1. $H + H + M \leftrightarrow H_2 + M^a$	6.4×10^{17}	0.0	-1.0
2. $H + OH + M \leftrightarrow H_2O + M^b$	8.4×10^{21}	0.0	-2.0
3. $O + O + M \leftrightarrow O_2 + M^c$	1.9×10^{13}	-1790	0.0
4. $O + H + M \leftrightarrow OH + M^d$	3.62×10^{18}	0.0	-1.0
5. $O_2 + H \leftrightarrow O + OH$	2.2×10^{14}	16800	0.0
6. $H_2 + O \leftrightarrow H + OH$	1.8×10^{10}	8900	1.0
7. $H_2 + OH \leftrightarrow H_2O + H$	2.2×10^{13}	5150	0.0
8. $OH + OH \leftrightarrow H_2O + O$	6.3×10^{12}	1090	0.0

Third body efficiencies:
a. $O_2 = 1.5$, $H_2 = 4$, $H_2O = 10$, $OH = 25$, $H = 25$, $O = 25$
b. $O_2 = 6$, $H_2 = 5$, $H_2O = 17$, $OH = 12.5$, $H = 12.5$, $O = 12.5$
c. $O_2 = 11$, $H_2 = 5$, $H_2O = 5$, $OH = 12.5$, $H = 12.5$, $O = 12.5$
d. $O_2 = 5$, $H_2 = 5$, $H_2O = 5$, $OH = 12.5$, $H = 12.5$, $O = 12.5$

Table 1: Hydrogen/oxygen reduced mechanism. The quantities are expressed in cal, mol, K

2.2 Heat Transfer Model

As stated before the main purpose of this paper is to show the multi-species formulation introduced in EcosimPro with the new combustion chamber component. Therefore the implemented submodel for the heat transfer is inherited from the

$\rho_L\ [kg/m^3]$	$p_L[Pa]$	$u_L\ [m/s]$	$\rho_R\ [kg/m^3]$	$p_R\ [Pa]$	$u_R\ [m/s]$
0.16047	1.0	0	0.020059	0.1	0

Table 2: Initial Values for the Sod shock tube test

already existing combustion chamber component. The hot gas side heat transfer is hence calculated by means of the Bartz correlation [16].

3 Model Validation

3.1 Roe and AUSM scheme

To validate the results obtained with the new component a series of classical initial value problems has been conducted. In this paper the results for the Sod's shock tube test [17] are reported. The test concerns a straight tube domain with discontinuous initial conditions, where the jump in the thermodynamic properties is imposed for the sake of simplicity in the middle of the computational domain. The tube is filled with Helium at rest, the initial conditions are reported in Table 2.

With the imposed initial conditions a set of three waves is generated. As shown in Figures 1-3 the right travelling shock approaches the right end of the domain, while the left travelling expansion propagates slower than the shock towards the left end of the domain. The contact discontinuity follows the shock towards the right end of the domain, its position can be identified only in the density plot of Figure 3. The results for both the schemes are plotted in Figures 1 - 3 against the solution obtained with an exact Riemann solver. The test is performed for both first and third order accurate spatial reconstruction. Clearly the first order shows an expected dissipative behaviour, while the third order is able to accurately predict both the shock position and the front edge of the expansion fan. The differences in terms of accuracy between the two schemes can be considered negligible.

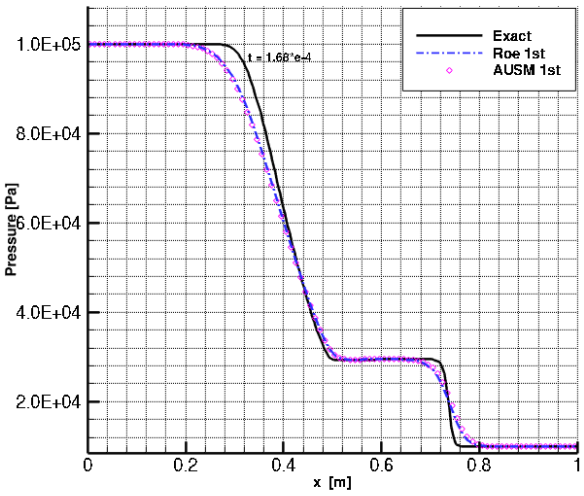

Figure 1: Pressure: Roe 1st order and AUSM 1st order vs exact solution

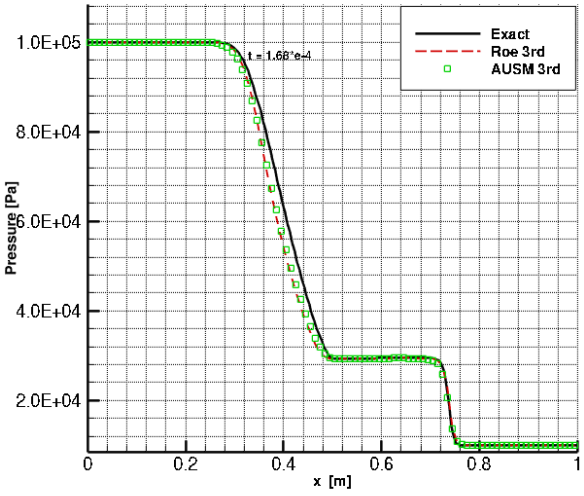

Figure 2: Pressure: Roe 3rd order and AUSM 3rd order vs exact solution

3.2 Finite Rate Model

The reduced scheme presented in Table 1 is here tested with two different test cases. The main goal of this section is to verify the capability of the new component in reaching a correct steady state solution. The first test case consists in a simple box: a straight tube with wall boundary conditions imposed on both boundaries and filled with a mixture of hydrogen and oxygen. In absence of a dedicated procedure to simulate the ignition phenomena, the initial total temperature conditions are such that the enthalpy content of the mixture is high enough to trigger the combustion process. The high temperature mixture is left to react and the results in terms of temperature and mass fractions are compared with the ones obtained from the assigned internal energy and volume problem in CEA [12]. Three different mixture ratios are tested, namely: stoichiometric (O/F = 8), ox-rich (O/F = 10.66) and fuel-rich (O/F = 5.33). The assigned initial conditions of pressure and temperature are respectively 1 bar and 1000 K. Being the fluid at rest this first test case gives information only on the finite-rate terms contribution. To test both the finite-rate and convective terms influence on the solution, a second test is performed. In this case the duct is open on both ends and a constant mass flow of 2.54 kg/s is imposed. The tube is characterized by a length $L = 0.4\ m$ and a diameter $D = 0.25\ m$. The reactants enter the domain at high temperature (1000 K) and evolve into products increasing both temperature and pressure in the duct. The resulting thermodynamic equilibrium state is then compared with the results

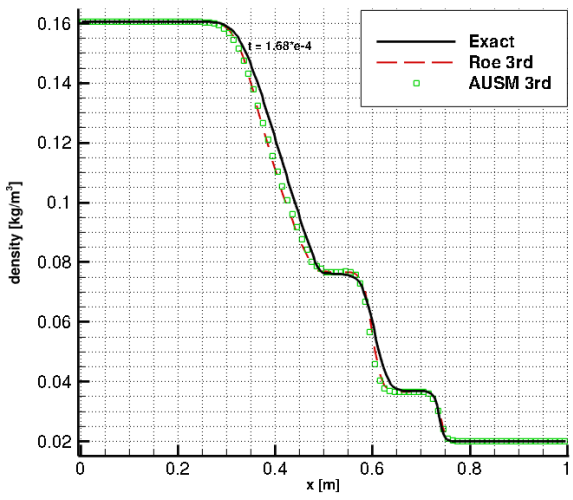

Figure 3: Density: Roe 3rd order and AUSM 3rd order vs exact solution

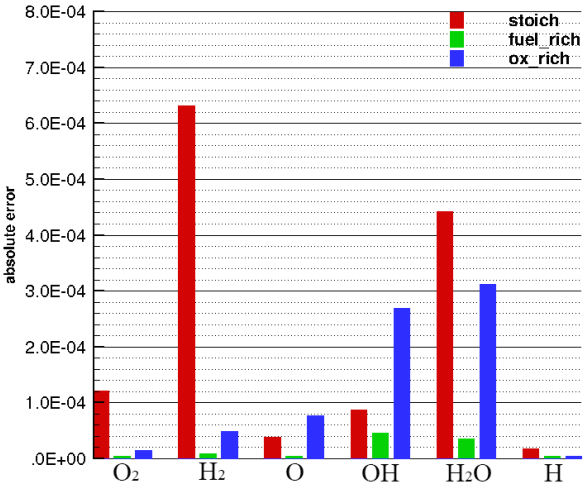

Figure 5: Absolute errors of mass fractions, pressure and temperature for the constant pressure test

obtained from the assigned enthalpy and pressure problem in CEA. The assigned pressure values are 36.03 bar, 35.58 bar and 35.42 bar respectively for the stoichiometric, fuel-rich and ox-rich test case. The results in terms of absolute mass

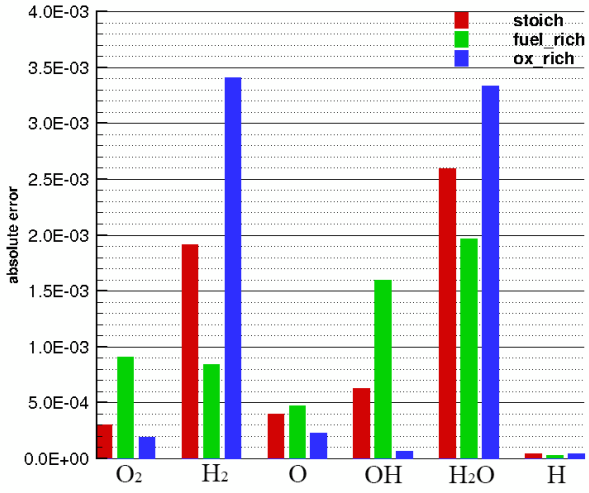

Figure 4: Absolute errors of mass fractions, pressure and temperature for the constant volume test

fraction errors are shown in Figure 4 and in Figure 5. For the constant volume test case the main difference is registered for the molecular hydrogen mass fraction in the fuel rich case. A strong dependence of the errors on the mixture ratio is noticed and a general trend cannot be distinguished. The error on the equilibrium condition is due to the nature of the reduced mechanism. Being the mechanism suited for high-pressure combustion processes a possible reason for the registered discrepancies can be found in the low pressure imposed as initial condition. This hypothesis is supported by the results carried out for the second test cases, where lower errors are registered. In both cases equilibrium temperatures reached with the present mechanism are in good agreement with the ones obtained from CEA, with a maximum difference of 0.156% registered in the box test case for the fuel rich configuration.

4 SSME Test Case

The new component has finally been tested on an existing combustion chamber. In this way the Q1D formulation is validated together with the finite-rate chemistry sub-model. The test case refers to the Space Shuttle Main Engine (SSME) Main Combustion Chamber (MCC) at Full Power Level (FPL, 109% of rated thrust). The SSME is a LOX/hydrogen staged-combustion engine with a regenerative cooling system that uses the fuel as coolant. In absence of an ignition procedure the combustion products are injected directly in the combustion chamber component. The composition of the inlet mixture is taken from the CEA equilibrium calculation for the FPL operative conditions, characterized by a chamber pressure $p_c = 225.87\ bar$ and a mixture ratio $O/F = 6$. The divergent section of the nozzle is simulated up to an area ratio of 5.00, hence cutting the last part of the divergent section that in the actual engine reaches an overall area ratio of 77.5. This choice was made to reduce the number of points in the grid while retaining a good resolution on the analysed part of the thrust chamber. In the present analyses the Roe's scheme is used with a third order accurate spatial reconstruction. The obtained results are then compared with the ones computed by TDK. The latter is able to analyse the steady-state flow evo-

lution inside the diverging section by means of a conjugated use of the method of characteristics (MOC) and the finite-rate chemistry. The MOC can only be applied to regions where the flow is supersonic, hence for the subsonic part the tool adopts a quasi one dimensional model. Aside of the two-dimensional solution TDK gives also a quasi one dimensional solution for the supersonic part. The one dimensional solutions for the subsonic and supersonic sections will be compared with the combustion chamber component. Simulations are carried out for two different cases: frozen and non-equilibrium flow. For the non-equilibrium case, TDK assumes the flow in chemical equilibrium up to the throat and applies the finite-rate model only in the supersonic region. This assumption is valid because in the converging section the characteristic times for the chemistry are smaller if compared to those of convection, hence the flow can be reasonably assumed in chemical equilibrium. At first the solution obtained with EcosimPro for the frozen case is compared with the reference one for different levels of spatial discretization. The scope is to investigate the optimal spatial discretization in terms of accuracy of the computed solution and time elapsed in the simulation. Three different configurations have been tested with respectively 20, 40 and 60 nodes. The results shown in Figures 6 and 7 highlight a satisfactory agreement in terms pressure and temperature evolution. The main difference is registered between the 20 nodes and the 40 nodes solution, a further increase from 40 to 60 nodes reduces the errors of less than one percentage point (0.6 achieved in the throat region for the temperature). The configuration with 40 nodes is thus chosen to compare the combustion chamber component with TDK. The results for the frozen case are proposed together with the ones with finite-rate chemistry to highlight the differences between the two flow configurations. The results in Figures 8 and 9

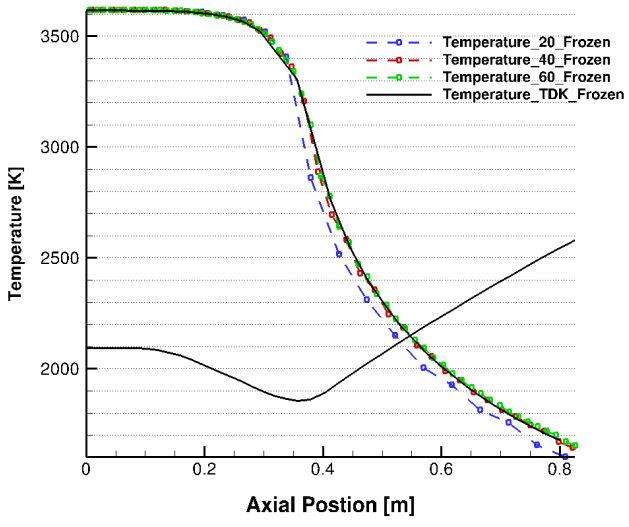

Figure 6: Temperature evolution for different grid levels vs TDK solution

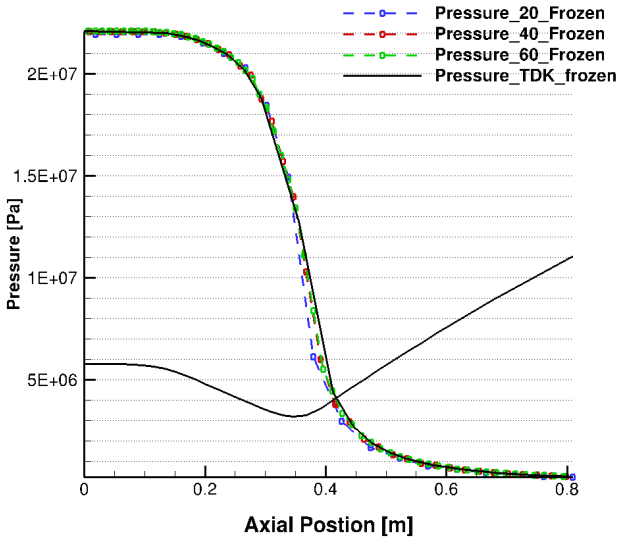

Figure 7: Pressure evolution for different grid levels vs TDK solution

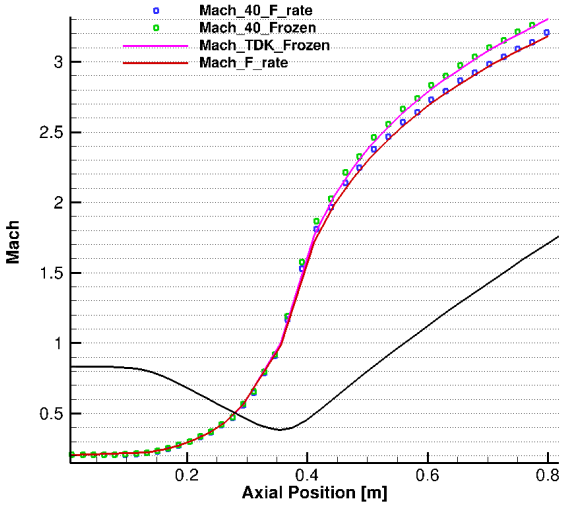

Figure 8: Mach number evolution: Combustion chamber component vs TDK solution

show a satisfactory agreement between the computed solution and the reference one. For both Mach and temperature the maximum difference in the finite-rate case is registered in the first part of the diverging section. The percentage errors are 2.56 and 0.95 points respectively for Mach number and temperature. In order to reduce the error a finer grid should be used, with the related drawback of an increased computational time. Anyhow, the reached accuracy can be considered acceptable for a system analysis tool. In the case with finite-rate chemistry the presence of exothermic recombination reactions causes an increase in the temperature values. The evo-

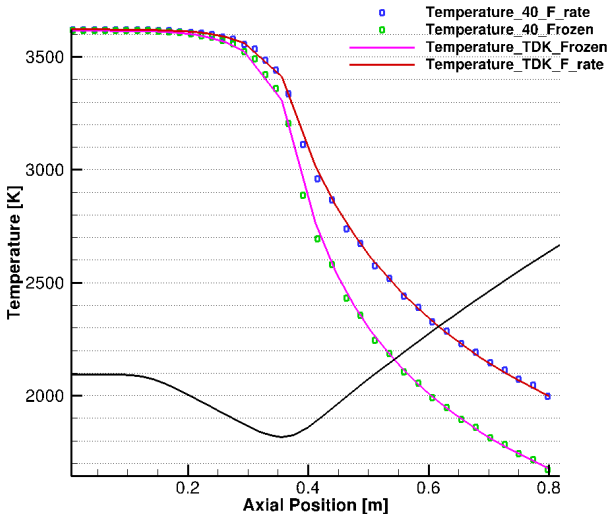

Figure 9: Temperature evolution: Combustion chamber component vs TDK solution

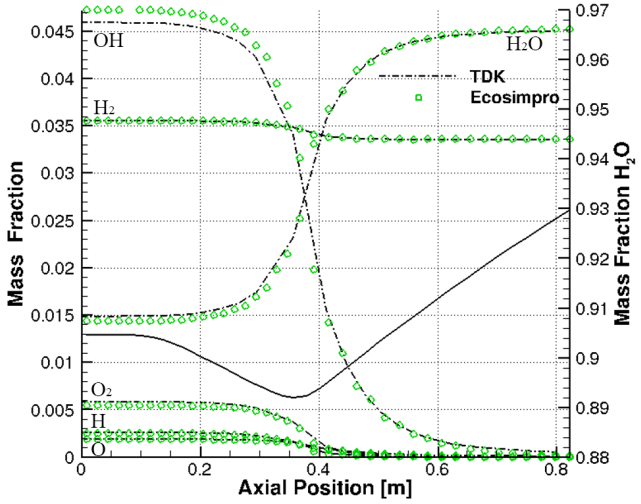

Figure 10: Mass fraction evolution: Combustion chamber component vs TDK solution

lution of the species in the whole domain is reported in Figure 10, where the H_2O concentration is showed on the secondary axis. A general good agreement is observed, in terms of spatial evolution of the species. The main difference between EcosimPro and TDK is registered for the H_2 concentration with a percentage difference of 2.5 points. This discrepancy is ascribed to the temperature difference between EcosimPro and TDK.

5 Conclusion

A new combustion chamber component for unsteady flow in chemical non-equilibrium has been presented and validated. The new component extends the present modelling capabilities of EcosimPro by means of a more accurate representation of the wave propagation and combustion processes. The implemented schemes, namely the Roe and AUSM scheme, exhibit almost the same behaviour in terms of accuracy of the computed solution. Furthermore, the component is capable to reproduce in a satisfactory way the evolution of both thermodynamic properties and mixture composition when applied to existing thrust chambers. The formulation of the new component is such that the user can easily add his own mechanism in EcosimPro, in order to simulate combustion processes involving a different propellant combination from the one proposed. Anyway attention must be payed to the number of species that the new mechanism will introduce. In fact, as noticed in section 4, a minimum number of nodes is required to reach an accurate description of the flow field inside the thrust chamber. Hence mechanisms involving a relatively low number of species should be preferred, in order to avoid an excessively high number of equations. In this way the overall number of variables for the combustion chamber component can be lowered, limiting the computational time when dealing with the analysis of complete systems.

Despite the steady-state validation test cases the proposed component is in principle able to analyse unsteady phenomena. However the present formulation lacks of an adequate procedure to simulate the ignition transients. The future work will be focused on devising and implementing a suitable model to properly reproduce the ignition procedure. This final step will complete the combustion chamber component, enabling the analysis of the typical transient processes in liquid rocket engines.

Acknowledgments

The present work has been conducted in the frame of the Network Partnering Initiative agreement between the European Space Agency (ESA) and the Dipartimento di Ingegneria Meccanica e Aerospaziale (DIMA) of University of Rome ‘La Sapienza ’.

References

[1] Empresarios Agrupados, “EcosimPro: Continuous and Discrete Modelling Simulation Software,” http://www.ecosimpro.com, 2007.

[2] Empresarios Agrupados, “ESPSS User Manual,” 2.4 edition, 2012.

[3] Di Matteo, F., De Rosa, M., and Onofri, M., “Transient Simulation of the RL-10A-3-3A Rocket Engine,” *Space*

Propulsion Conference 2012, edited by 3AF, 2012, Abstract submitted for the Space Propulsion Conference 2012.

[4] Isselhorst, A., "HM7B Simulation with ESPSS Tool on ARIANE 5 ESC-A Upper Stage," *46th AIAA/ASME/SAE/ASEE Joint Propulsion Conference and Exhibit*, No. AIAA 2010-7047, 2010.

[5] Roe, P., "Approximate Riemann solvers, parameter vectors, and difference schemes," *J. Comput. Phys.*, Vol. 43, 1981, pp. 357–372.

[6] Liou, M.-S., "A sequel to AUSM, Part II: AUSM$^+$-up for all speeds," *Journal of Computational Physics*, Vol. 214, No. 1, 2006, pp. 137 – 170.

[7] Petzold, L. R., "A Description of DASSL: A Differential/Algebraic System Solver," Tech. rep., Sandia National Laboratories report SAND82-8637, 1982.

[8] Nickerson, G. R., Dang, L. D., Coats, E. E., and Center, G. C. M. S. F., "Engineering and programming manual: two-dimensional kinetic reference computer program (TDK) / by G. R. Nickerson, L. D. Dang, E. E. Coats. [microform]," 1985, "Final report.".

[9] Cinnella, P., *Flux-Split Algorithms for flows with non-equilibrium chemistry and thermodynamics*, Ph.D. thesis, Virginia Polytechnic Institute and State University, Blacksburg, December 1989.

[10] Liou, M.-S. and Jr., C. J. S., "A New Flux Splitting Scheme," *Journal of Computational Physics*, Vol. 107, No. 1, 1993, pp. 23 – 39.

[11] Liou, M.-S., Edwards, J. R., and Center., N. G. R., *Numerical speed of sound and its application to schemes for all speeds*, National Aeronautics and Space Administration, Glenn Research Center , National Technical Information Servicecinnell, 1999.

[12] Gordon, S. and McBride, B. J., "Computer Program for Calculation of Complex Chemical Equilibrium Compositions and Applications," Tech. Rep. RP-1311, NASA, 1994.

[13] Baulch, D. L., Cox, R. A., Crutzen, P. J., Hampson, Jr., R. F., Kerr, J. A., Troe, J., and Watson, R. T., "Evaluated Kinetic and Photochemical Data for Atmpospheric Chemistry," *J. Phys. Chem*, Vol. Ref. Data 11, 1982, pp. 327–496.

[14] Jensen, D. and Jones, G., "Reaction rate coefficients for flame calculations," *Combustion and Flame*, Vol. 32, No. 0, 1978, pp. 1 – 34.

[15] Baulch, D., Bowers, M., Malcolm, D., and Tuckerman, R., "Evaluated Kinetic Data for High-Temperature Reactions," *J. Phys. Chem*, Vol. 15, N.2, 1986, pp. 465–592.

[16] Bartz, D. R., "Turbulent Boundary-Layer Heat Transfer from Rapidly Accelerating Flow of Rocket Combustion Gases and of Heated Air," Tech. Rep. NASA-CR-62615, Jet Propulsion Laboratory, 1963.

[17] Toro, E. F., *Riemann Solvers and Numerical Methods for Fluid Dynamics: a Practical Introduction*, Springer, 1999.